From Dish to Tissue: Developing Melanoma Tumors in Bioengineered Human Skin Equivalents

Felikss Rumnieks[1,2], Deniz Ornek[2], Hasan Erbil Abaci[2]

(1) Latvian Biomedical Research and Study Centre, Riga, Latvia; (2) Columbia University Irving Medical Centre Department of Dermatology, New York, USA; #correspondence: felikss.rumnieks@biomed.lu.lv

Introduction:

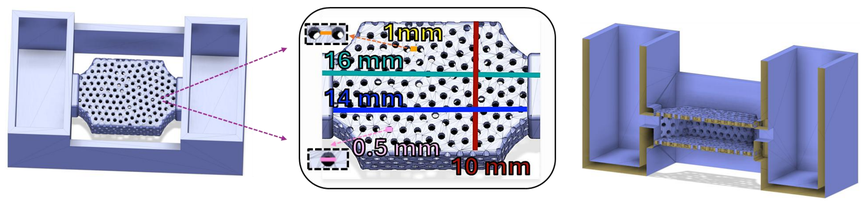
Melanoma, a highly aggressive skin cancer, develops within a complex microenvironment that conventional 2D cultures fail to replicate. To better model tumor–stroma interactions and therapeutic responses, we established bioengineered edgeless human skin equivalents incorporating reconstructed melanoma tumors (MeWo, A375). These 3D models recapitulate key features of native skin architecture, including dermis, epidermis, and tumor mass. Through histological and immunofluorescent analyses, we examined tumor organization, stromal activation, and microvascular integration. Finally, we evaluated treatment responses to BRAF and MEK inhibitors by changes in proliferative activity, demonstrating the platform's potential for translational melanoma research.

Aim:

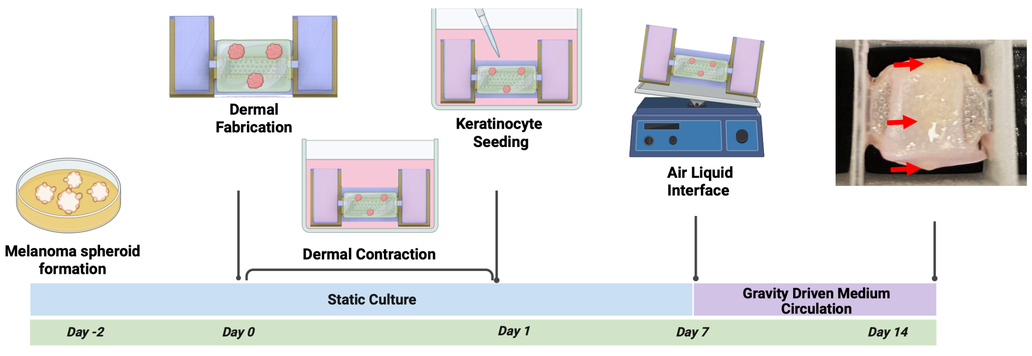
To engineer a human skin equivalent containing vascular and melanoma components for functional analysis of early metastasis and drug efficacy.

Methods

CAD Design and 3D Printing of the Chip:



Fabrication of the Edgeless Human Skin Melanoma Chip:



Following the proliferation and maturation/differentiation phases, constructs were fixed and processed for downstream analysis. Samples were either paraffin-embedded for histological staining or embedded for cryosectioning to enable immunofluorescence applications. Resulting sections were analyzed using histological and immunofluorescent techniques to assess tissue architecture, cellular organization, and marker expression.

Results:

Macroscopic and histological characterization

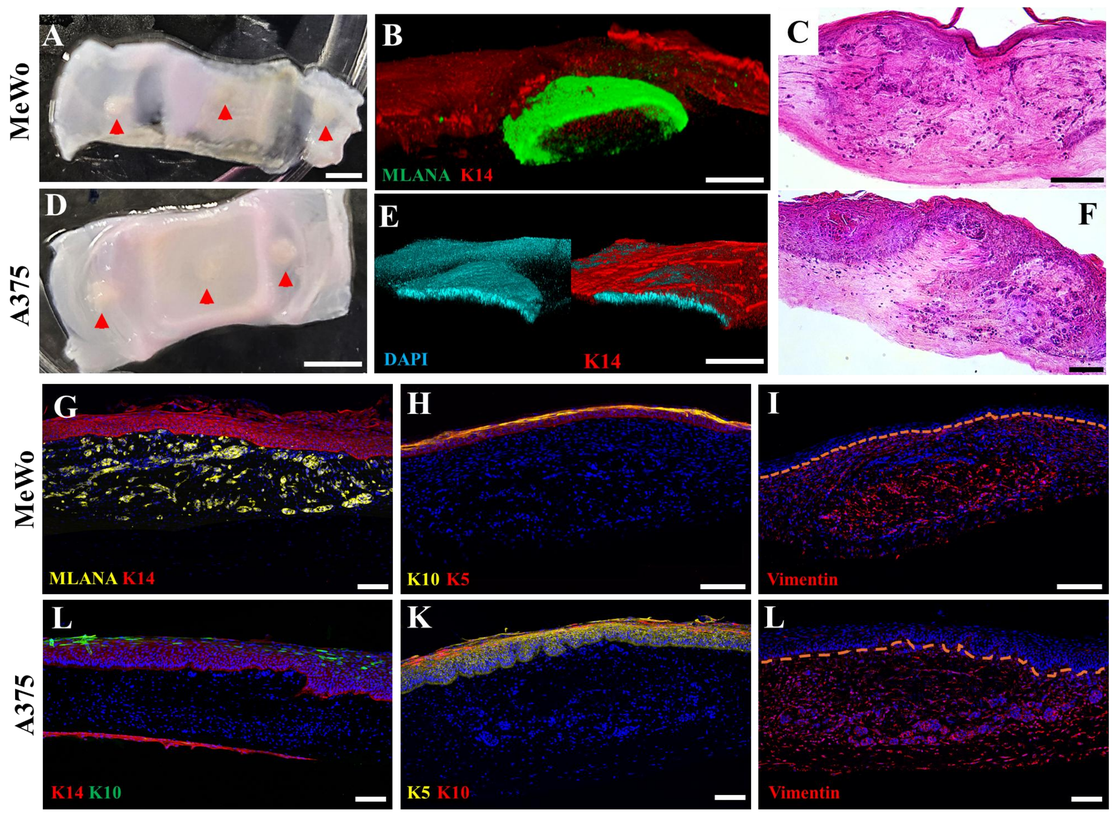


Figure 1. (A,D) Macroscopic appearance of the edgless human skin melanoma equivalents; **(B,E)** Whole-mount immunostained 3D confocal images visualizing the tumor mass and epidermal keratin (K14) distribution (Scale bar: 250µm). **(C, F)** H&E-stained sections showing distinct dermal and epidermal layers with an integrated tumor mass (Scale bar: 250µm); **(G-L)** cross-sections depicting epidermal and dermal markers of the edgless models. Scale bar: 5mm (A, D); 250µm (B,E,G-L)

Endothelial cell introduction into the model

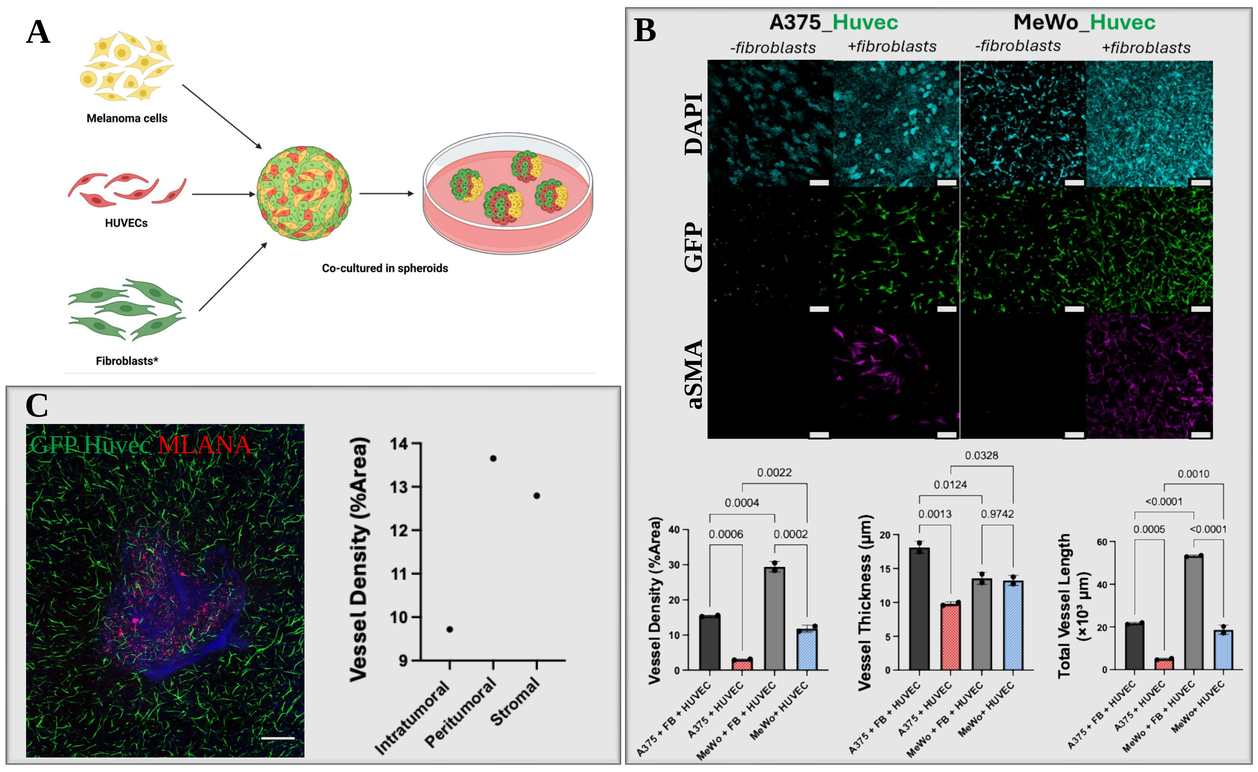


Figure 3. (A) Schematic of vascularized reconstructed tumor formation; **(B)** Dermal fibroblasts (FBs) facilitate microvascular network formation within the tumor spheroids (Scale bar: 200µm) **(C)** Whole-mount confocal image of the vascularized edgless melanoma model (Scale bar: 500µm)

Tumor microenvironment:

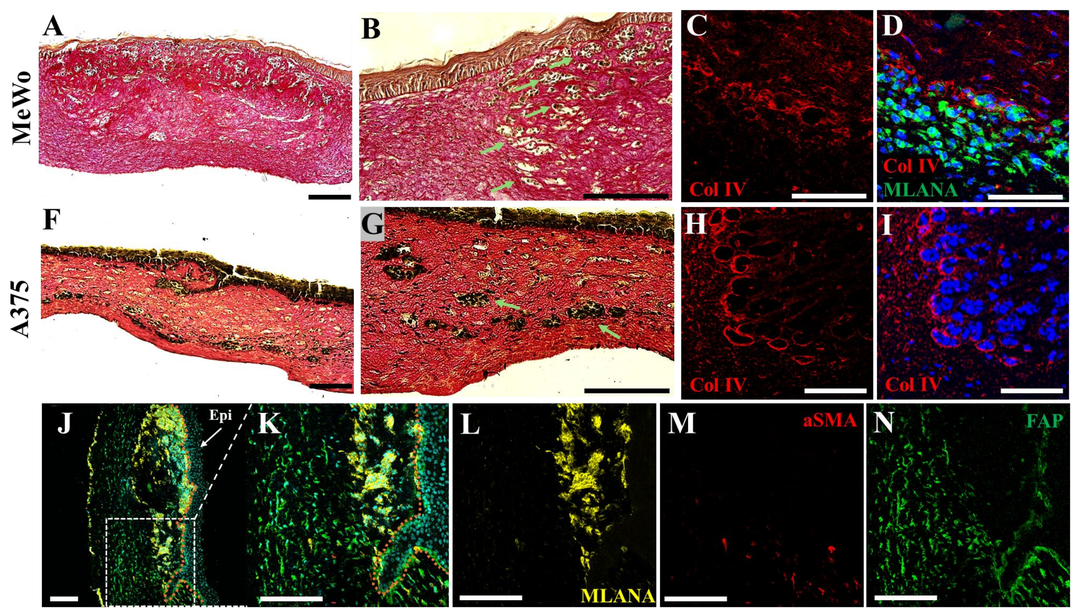


Figure 2. (A-B; F-G) Picrosirius staining reveals contrast of collagen fiber polarization between tumor mass (unpolarized) and dermis (polarized), and show matastatic cyst-like formations ath the perifery of the tumor mass (arrows); **(C-D; H-I)** The metastaic cyst-like formations at the perifery of the tumor mass are positive for Callagen IV; **(J-N)** Cancer associated fibroblasts reside in the proximity of the tumor. Scale bars: 200µm (A-B; F-G; J-N); 100µm (C-D; H-I)

Melanoma cell proliferation rate declines after drug treatment

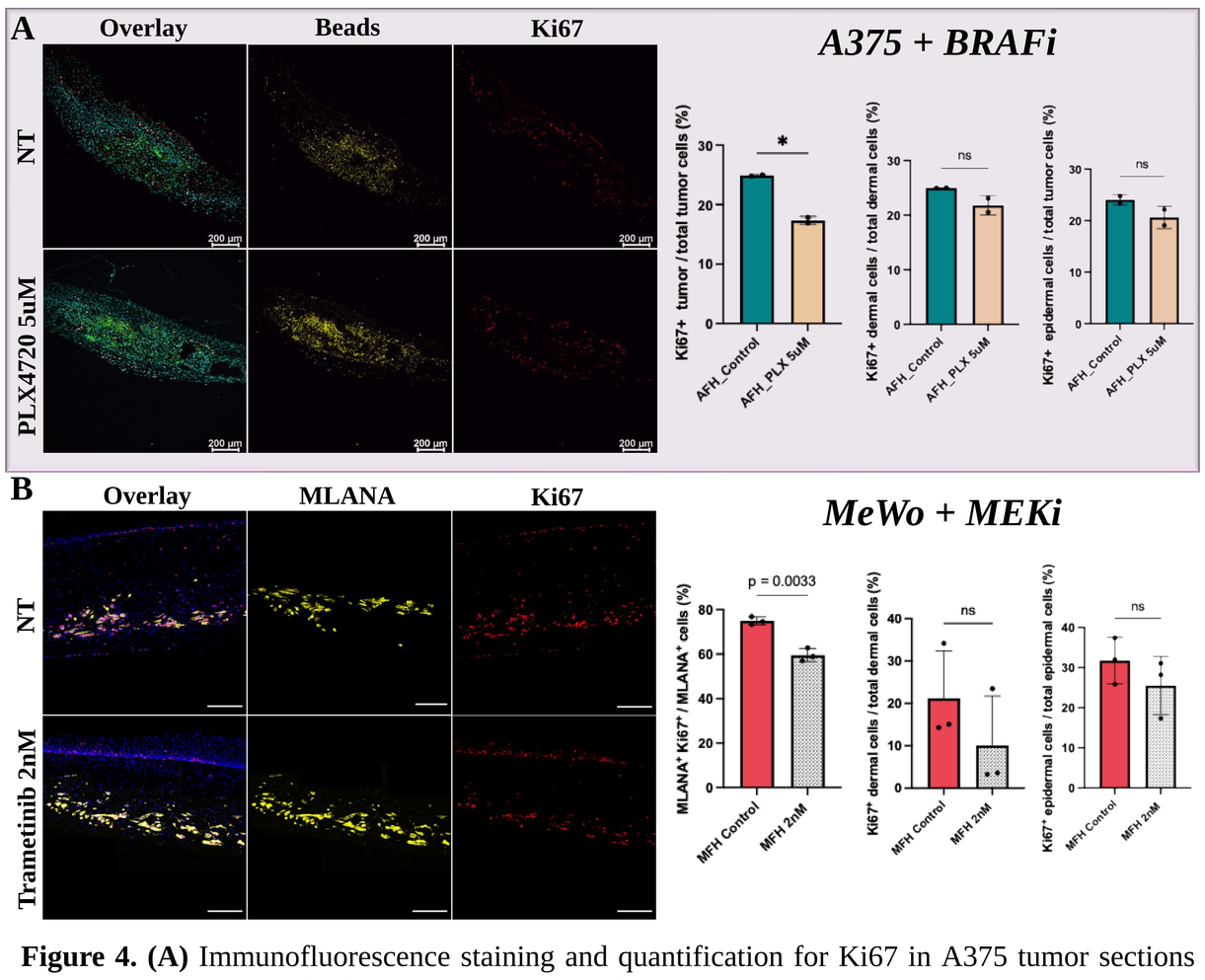


Figure 4. (A) Immunofluorescence staining and quantification for Ki67 in A375 tumor sections comparing non-treated (NT) and PLX4720 (5 µM)–treated constructs.
(B) Ki67 staining and quantification of MeWo tumor sections following Trametinib treatment 2 nM or left untreated (NT).
All treatments were applied for seven days prior to fixation. Scale bars: 200µm